• Investigation •

Topographic distribution features of the choroidal and retinal nerve fiber layer thickness in Wenzhou school-aged children

Wei-Qin Liu[1,2], *Dan-Dan Wang*[1,2], *Xiao-Xia Yang*[1,2], *Yan-Yan Pan*[1,2], *Xue Song*[1,2], *Yu-Shan Hou*[1,2], *Chen-Xiao Wang*[1]

[1]Eye Hospital of Wenzhou Medical University, Wenzhou 325027, Zhejiang Province, China
[2]Optometry Academy of Wenzhou Medical University, Wenzhou 325027, Zhejiang Province, China
Correspondence: Chen-Xiao Wang. The Eye Hospital, Wenzhou Medical University, 270 Xueyuan Road, Wenzhou 325027, Zhejiang Province, China. chenxiaow@outlook.com
Received: 2019-05-20 Accepted: 2020-01-20

Abstract

● **AIM:** To explore the topographic distribution features of choroidal thickness (CT) and retinal nerve fiber layer thickness (RNFLT), and determine the relationship between CT and ocular parameters in school-aged children.

● **METHODS:** The healthy school-aged children with low myopia or emmetropia in Wenzhou were recruited for this cross-sectional study. With high-density optical coherence tomography (HD-OCT) combined with MATLAB software, the CT and RNFLT values in the macular area were measured at different locations and compared. Statistical analyses were performed to evaluate the correlation between CT and ophthalmic parameters, such as spherical equivalent (SE) and the axial length (AL).

● **RESULTS:** A total of 279 school-aged children with 8.00±1.35 years of mean age (range, 6-10y) were included. The mean AL was 23.66±0.86 mm. The mean CT in CT-C (264.31±48.93 μm) was thicker than that in CT-N1 (249.54±50.52 μm), and the average CT in the parafoveal region was also thicker than that in CT-N2 (235.65±50.63 μm). The subfoveal CT also varied substantially across refractive errors (P<0.001), and those with myopia (250.59±47.01 μm) exhibited a thinner choroid compared with those with emmetropia (278.74±48.06 μm). CT positively correlated with AL (y=11.12x-4.15; R^2=0.18), and positively correlated with SE (y=90.07x+17.916; R^2=14.2). The average RNFLT was thickest in the peripapillary region (236.35±19.03 μm), the mean RNFLT-S (131.10±15.16 μm) was thicker than the RNFLT-I (128.20±16.59 μm), and the mean RNFLT-T (76.54±11.99 μm) was thicker than the RNFLT-N (64.28±8.55 μm). The variations in the RNFLT between quadrants did differ between those with myopia and emmetropia (P<0.05).

● **CONCLUSION:** We establish demographic information for the choroid and RNFLT. These findings provide information that should be considered in future analyses of the CT and RNFLT in OCT studies in school-aged children.

● **KEYWORDS:** children; choroid; myopia; refractive error; retinal nerve fiber layer; optical coherence tomography
DOI:10.18240/ijo.2020.03.15

Citation: Liu WQ, Wang DD, Yang XX, Pan YY, Song X, Hou YS, Wang CX. Topographic distribution features of the choroidal and retinal nerve fiber layer thickness in Wenzhou school-aged children. *Int J Ophthalmol* 2020;13(3):466-473

INTRODUCTION

Structural and functional abnormalities of the choroid are likely to contribute to major ocular diseases[1], and the choroid plays a clinically significant role in the pathological mechanisms of oculopathy[1-2]. The choroid also plays a role in the long-term progression of refractive errors, as demonstrated by the finding that it acts as a medium in the visual signaling pathways between the retina and sclera in animal models and humans[2-3]. The incidence rate of myopia has increased in recent years, and at present, the highest rate of this disease is found in East Asia, where rates up to 70%-90% among young adults have been detected in countries such as Singapore and China[4-5]. Myopia has emerged as a major global public health issue, and predictions have indicated that nearly five billion people throughout the world will have myopia in 2050[6]. Studies on optical corrections imposed by orthokeratology treatment in the cornea of children have provided favorable evidence for the control of myopia progression characterized by increases in the choroidal thickness (CT)[7].

Imaging of the myopic eye is crucial for the diagnosis of sight-threatening complications, the assessment of treatments and the monitoring of disease development. In the last decade, the invention of optical coherence tomography (OCT), which allows high-resolution imaging of the choroid, was a

momentous revolution in ocular imaging and corresponding changed the available treatments in clinical ophthalmology. In addition, this technique enhanced the quality of the obtained choroid images, which allows a convenient approach for the simple and accurate measurement of the CT and expands our understanding of the pathogenesis of myopia[8-9].

A large number of studies have surveyed the CT in healthy participants and have primarily focused on the macular region, which is the most sensitive part of the human eye and the location where the choroid provides nutrients and oxygen[10]. Recent research has focused on the choroid, which is an indispensable structure in the pathophysiology and pathomechanism of amblyopia and emmetropization. Amblyopia has long been known as a cortical disease, but the depth of cognition associated with this complex pathomechanism is limited[11-12]. Thinning of the choroid, which is associated with an extension of the axial length (AL) and myopic shift, has been affirmed in myopic progression[13]. The diagnosis of children's eye diseases, such as strabismus, amblyopia and pathological myopia, requires a structural database based on children as a reference. However, clinical studies on the choroid in emmetropes are very rare. Therefore, an understanding of the normal baseline CT and retinal nerve fiber layer thickness (RNFLT) derived from a population-based study is crucial for future studies.

SUBJECTS AND METHODS

Ethical Approval This study was supported by the Ethics Committee of Eye Hospital and abided by the tenets of the Declaration of Helsinki. Written informed consent and oral consent were acquired from the parents or guardians and the children before the research was formally implemented.

Participants This cross-sectional investigation was a population-based study, and children belonging to a Chinese Han population were consecutively recruited for this study from January 2016 to September 2018 at Eye Hospital of Wenzhou Medical University. The guardians or parents of the children completed a strictly standardized questionnaire that contained questions regarding their occupation, educational background and earnings. A total of 279 participants were included and underwent a full-scale ophthalmic examination that included assessments of the intraocular pressure (IOP), refractive error, and best-corrected visual acuity (BCVA), which was converted into logMAR, slit-lamp examination, and imaging tests, including fundus photography and high-density optical coherence tomography (HD-OCT; Carl Zeiss Meditec Inc., Dublin, CA, USA). Systemic biological indexes of the children, such as the height and weight, were determined. The children were subjected to analyses of subjective refraction without cycloplegia by practiced optometrists. The spherical equivalent (SE) was equivalent to half a cylinder plus the sphere. The AL was measured using a Lenstar LS900 measuring instrument (Lenstar LS900), which was developed by the Swiss company Haag-Streit and the German company Wavelight. The inclusion criteria were as follows: aged 6 and 10y; SE less than 3.0 D; IOP less than 21 mm Hg; normal anterior chamber angle and BCVA; and normal fundus appearance on OCT examination. Participants with a history of disease, including hypertension, diabetes, congenital cataract, congenital glaucoma, intraocular injections or surgery, refractive surgery, and other clues of oculopathy, were also eliminated by trained ophthalmologists and questionnaires.

HD-OCT Imaging The HD-OCT (Carl Zeiss Meditec Inc., Dublin, CA, USA) system was applied to image the retina and choroid using a scanning speed of 27 000 A-scans per second with a 480-nm wavelength optical source. Images of the vitreoretinal junction adjacent to the zero-delay were obtained[14-16]. Each eye underwent circle scans around the optic nerve with a circle size of 3.46 mm. The mean RNFLT was obtained and automatically recorded using built-in software. The RNFLT was equivalent to the vertical distance from the intimal limiting membrane (ILM) to the retinal ganglion cell layer. The average RNFLT of the macular fovea and the thickness in the inferior, superior, temporal and nasal surrounding areas were recorded as RNFLT, RNFLT-I, RNFLT-S, RNFLT-T and RNFLT-N, respectively. The CT was equivalent to the vertical distance from the choroidal-scleral interface to Bruch's membrane, and the macular CT was defined as the CT at the foveal center. The five-line raster model of the HD-OCT was also used for a manual estimation of the CT, and CT values were detected at five sites in different regions of the subjects, including the macular fovea and 500 and 1000 μm from the macular region at the naso-temporal sites (CT-C, CT-N1, CT-N2, CT-T1, and CT-T2, respectively). Scans of the right eye were performed first, and the results of the scans were evaluated by trained clinical technicians who performed the ophthalmological diagnosis of the participants and did not participate in the statistical analysis of the data. All examinations were performed under strict standardized circumstances and at a uniform time period (8:00-16:00) to lessen the diurnal variation in the CT[17].

The CT measurements were calibrated using MATLAB (MathWorks Inc., USA). The AL was imported into the software to modulate the amplification factors resulting from the AL, and the average value and its consistency was obtained after three repeated measurements (Figure 1A)[18]. Images of both eyes with a signal strength index less than or equal to 6/10 were excluded. The results for the first 48 participants obtained were analyzed twice to examine the reproducibility of the CT measurements. The Bland-Altman plots comparing the CT measurements obtained by two experienced doctors are shown in Figure 1B.

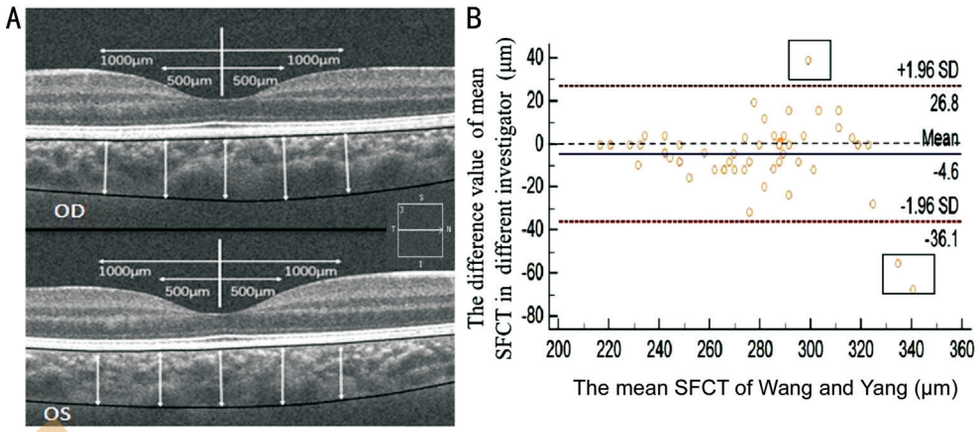

Figure 1 Horizontal image of the choroid obtained by HD-OCT A: The boundaries and thickness profiles of the choroid were obtained in the inner region (ranging from 500 to 1000 μm of eccentricity) by HD-OCT combined with MATLAB programming; B: The Bland-Altman plot of the consistency of the subfoveal choroidal thickness (SFCT) values measured by two experienced ophthalmologists (Wang DD and Yang XX; *n*=48).

Table 1 General information of the study population

Age (y)	Male, *n* (%)	BMI (kg/m^2)	Spherical equivalent, diopter		AL (mm)
			OD	OS	
6	54 (19.4)	16.50±2.14	-0.07±0.72	-0.04±0.63	23.23±0.70
7	61 (21.9)	16.27±2.12	0.43±0.85	0.43±0.90	23.47±0.83
8	63 (22.6)	19.22±16.52	-0.33±0.64	-0.32±0.70	23.53±0.76
9	55 (19.7)	17.26±2.56	-0.97±0.86	-0.94±0.90	24.07±0.83
10	46 (16.5)	17.65±2.32	-1.13±1.00	-1.10±1.05	24.14±0.78
Total	279	17.41±8.15	-0.56±0.90	-0.54±0.92	23.66±0.86

BMI: Body mass index; OS: Left eye; OD: Right eye; AL: Axial length.

Statistical Analysis All data were obtained in a double-blind manner and tested by two independent researchers. The statistical analyses were performed using SPSS 22.0 (SPSS Inc., Chicago, IL, USA). The normality of the distributions of the parameter variables was detected by the Kolmogorov-Smirnov test. The CT was expressed using extremum. The repeatability of the CT was evaluated by the concordance correlation coefficient with a 95% confidence interval (CI). Linear regressions were used to examine the associations between the CT and eye parameters, such as AL and SE. The correlation between CT and AL was analyzed by Pearson correlation analysis, and the correlations between CT and sex, diopter, age, and body mass index (BMI) were analyzed by Spearman rank correlation analysis. The statistical significance in all the tests was uniformly defined as P<0.05 (two-sided).

RESULTS

Overall Characteristics of the Participators Thirty-two of the 313 subjects recruited in this study were eliminated due to poor HD-OCT images. A total of 279 (89.1%) students with an average age of 8.00±1.35y (range, 6-10y) were included in the analysis, and 121 (43.4%) and 158 (56.6%) of these students were boys and girls, respectively. Fifty-four participants belonged to the 6-year-old group (19.4%), 61 participants belonged to the 7-year-old group (21.9%), 63 participants belonged to the 8-year-old group (22.6%), 55 participants belonged to the 9-year-old group (19.7%), and 46 participants belonged to the 10-year-old group (16.5%). The mean SE was -0.54±0.88 D, and the mean AL was 23.66±0.86 mm. Comprehensive information is presented in Table 1. The refractive error of the subjects was divided into myopia (45.5%), emmetropia (47%) and hyperopia (7.5%), and the SE ranged from -2.75 to +1.0 D. The mean weight, height and BMI were 7.92±1.35 kg, 131.73±8.78 cm, and 17.41±8.15 kg/m^2, respectively. The clinical validity of any apparatus depends on the reproducibility of its measurements; thus, a Bland-Altman plot was prepared to evaluate the individual variations in the CT measurements (*n*=48). In addition, an interesting tendency toward greater bias was obtained with greater CT values, and we can thus speculate that a thicker choroid makes the interface of the choroid sclera junction more difficult to discern (Figure 1B).

Topographic Distribution Features of CT and RNFLT The average RNFLT was thickest in the macular fovea (236.35±19.03 μm), the mean RNFLT-S (131.10±15.16 μm) was thicker than the RNFLT-I (128.20±16.59 μm), and the mean RNFLT-T (76.54±11.99 μm) was thicker than the RNFLT-N (64.28±8.55 μm). The mean CT in CT-C (264.31±48.93 μm) was thicker than that in CT-N1 (249.54±50.52 μm), and the

Table 2 General features of school-aged children μm

Parameters	Mean±standard deviation	Maximum	Minimum 95%CI
RNFLT	236.35±19.03	291.00	194.00 (164.90, 189.05)
RNFLT-S	131.10±15.16	184.00	91.000 (129.30, 132.88)
RNFLT-I	128.20±16.59	171.00	72 .000 (126.24, 130.16)
RNFLT-N	64.28±8.55	99.500	46.500 (75.080, 77.910)
RNFLT-T	76.54±11.99	131.50	48.000 (63.210, 65.510)
CT-N2	235.65±50.63	379.82	104.09 (229.47, 241.39)
CT-N1	249.54±50.52	391.63	107.04 (243.45, 255.37)
CT-C	264.31±48.93	411.31	125.95 (258.52, 270.08)
CT-T1	266.75±4.676	417.22	129.89 (261.04, 272.53)
CT-T2	269.39±47.32	419.18	139.30 (263.91, 275.07)

T1: Temporal sector 500 μm from the fovea; N1: Nasal sector 500 μm from the fovea; T2: Temporal sector 1000 μm from the fovea; N2: Nasal sector 1000 μm from the fovea; C: Macular fovea; CT: Choroidal thickness; RNFLT: Average thickness of the retinal nerve fiber layer; I: Inferior quadrant; S: Superior quadrant; T: Temporal quadrant; N: Nasal quadrant.

Table 3 Distribution differences in the RNFLT and CT in emmetropic and myopic children mean±SD, μm

Parameters (μm)	All subjects (n=260)	Emmetropia group (n=132)	Myopia group (n=128)
CT-N2	236.08±51.01	250.25±49.42	221.46±48.44[b]
CT-N1	249.96±50.96	264.46±49.11	235.01±48.44[b]
CT-C	264.88±49.59	278.74±48.06	250.59±47.01[b]
CT-T1	267.40±49.24	280.71±47.95	253.67±46.72[b]
CT-T2	131.40±15.29	133.95±13.97	128.77±16.13[a]
SFCT-U	131.40±15.29	133.95±13.97	128.77±16.13[a]
SFCT-D	128.04±16.20	131.02±16.32	124.97±15.49[a]
SFCT-N	64.38±8.77	65.95±9.59	62.75±7.49[a]
SFCT-T	76.62±12.00	76.42±9.96	76.82±13.78

RNFLT: Retinal nerve fiber layer thickness; CT: Choroidal thickness; T1: Temporal sector 500 μm from the fovea; N1: Nasal sector 500 μm from the fovea; T2: Temporal sector 1000 μm from the fovea; N2: Nasal sector 1000 μm from the fovea; C: Macular fovea; SFCT: Subfoveal choroidal thickness. The choroidal thickness of the myopic children was thinner than that of the emmetropic children. [a]P<0.05; [b]P<0.001.

average CT in the parafoveal region was also thicker than that in CT-N2 (235.65±50.63 μm; Table 2). The average CT decreased along the horizontal direction from the bitemporal to the nasal sector in the perifoveal region. The subfoveal CT in the macular area also varied substantially across refractive errors (P<0.001), and those with myopia (250.59±47.01 μm) exhibited a thinner choroid compared with those with emmetropia (278.74±48.06 μm). The variations in the RNFLT between quadrants did differ between those with myopia and emmetropia (P<0.05). Distinct thinning of the RNFLT was detected in those with myopia (Table 3).

The average CT in the central fovea of the macula obtained in our study (264.31±48.93 μm) was thinner than that obtained in other studies (251-337 μm)[19-20]. Interestingly, the variations in the choroid thickness in the posterior polar region were similar in different age groups (Figure 2), and this study constitutes the first assessment of these variations. The choroid was thickest in the central fovea of the macula, and the CT in the bitemporal region was somewhat thicker than that in the symmetrical

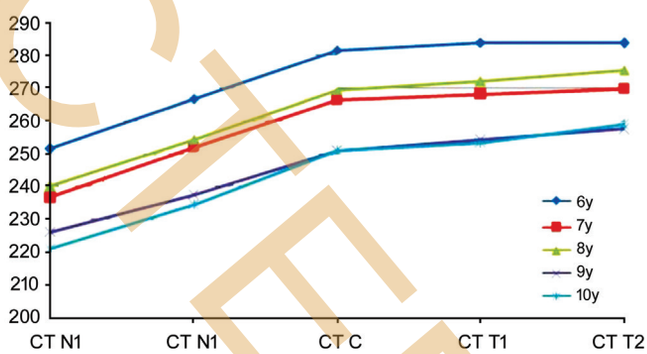

Figure 2 Line chart showing the CT at different sites in children aged 6 to 10y The mean thickness of the choroid was measured at 500-μm intervals from the macular fovea.

nasal region, which was consistent with previous studies[21-23]. To our knowledge, a subject's age, refractive status, race, and the apparatus and protocols utilized in the assessment might affect the accuracy of CT measurements. In our study, the average CT was measured and analyzed using MATLAB (MathWorks Inc., USA), and the AL was imported into the

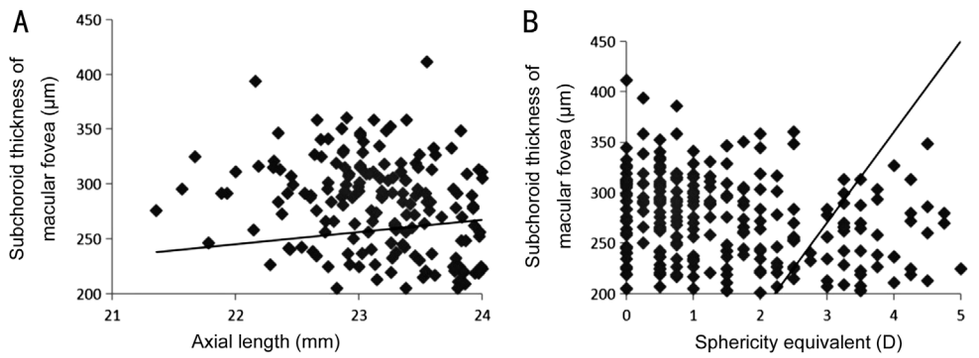

Figure 3 Linear correlation between the average macular CT and measurements of the AL and SE A: A moderate correlation was obtained (y=11.12x-4.15; R^2=0.18) with the SE across all the subjects; B: A correlation was obtained (y=90.07x+17.916; R^2=14.2) with the SE in all the subjects. *n*=279.

system to modulate the amplification effects caused by the AL. The average value and the consistency of the measurements were obtained after three repeated measurements, and our findings might yield a more accurate measurement of the CT in a Wenzhou population aged 6-10y. In addition, we performed correlation analyses of the factors affecting CT, such as age, sex, AL, and SE. The CT at different sites was correlated with age, sex, AL (Figure 3A), and RNFLT and CT were correlated with the SE (Figure 3B) and BMI, but these correlations were weak. The above-described research findings are demonstrated in detail in Tables 4-6.

DISCUSSION

The choroid is thought to be connected with the synthesis of sclera macromolecules and plays a role in controlling the growth of the eyeball and the occurrence of myopia and hyperopia. The currently study provides a basic reference range for CT measurements obtained by HD-OCT in Wenzhou school-aged children. To our knowledge, this study provides the first measurement of the baseline thickness of the choroid in Wenzhou school-aged volunteers obtained by HD-OCT and METLAB software and the first assessment of the relationships of the choroid with medical variables, including SE and thickness of the retina.

Due to advancements in OCT, such as faster processing software and scan speed, it is now possible to perform *in vivo* studies of the choroid to obtain in understanding of the dynamic process in the tissue[9,24]. Although many studies have focused on the CT in adults, scarce population- or school-based studies have provided data on the CT in children, which leads to potential referral-based bias. In addition, most studies have assessed the correlation between CT and age and included a low sample size of children with a wide age range[25-27]. Most studies on CT in children focused on comparisons of the CT between children and adults[28-29], and the CT in school-aged children with normal vision has rarely been reported. Overall, the growth and development of the choroid in school-

Table 4 Spearman rank correlation analysis of the CT with age and sex

CT	Age		Sex	
	P	*r*	*P*	*r*
CT-N2	0.001	-0.189[b]	0.051	-0.117
CT-N1	<0.0001	-0.209[b]	0.023	-0.136[a]
CT-C	<0.0001	-0.212[b]	0.019	-0.140[a]
CT-T2	0.001	-0.206[b]	0.028	-0.131[a]
CT-T1	0.003	-0.176[b]	0.088	-0.102

CT: Choroidal thickness; T1: Temporal sector 500 μm from the fovea; N1: Nasal sector 500 μm from the fovea; T2: Temporal sector 1000 μm from the fovea; N2: Nasal sector 1000 μm from the fovea; C: Macular fovea. [a]*P*<0.05; [b]*P*<0.01.

Table 5 Spearman rank correlation analysis of the CT with the BMI and SE

CT	SE, OD		SE, OS		BMI	
	P	*r*	*P*	*r*	*P*	*r*
CT-N2	<0.0001	0.282[b]	<0.0001	0.264[b]	0.740	0.020
CT-N1	<0.0001	0.282[b]	<0.0001	0.260[a]	0.835	-0.013
CT-C	<0.0001	0.272[b]	<0.0001	0.254[a]	0.951	0.004
CT-T2	<0.0001	0.264[b]	<0.0001	0.245[b]	0.843	0.012
CT-T1	<0.0001	0.225[b]	<0.0001	0.205[b]	0.756	0.019

CT: Choroidal thickness; SE: Spherical equivalent; BMI: Body mass index; T1: Temporal sector 500 μm from the fovea; N1: Nasal sector 500 μm from the fovea; T2: Temporal sector 1000 μm from the fovea; N2: Nasal sector 1000 μm from the fovea; C: Macular fovea. [a]*P*<0.05; [b]*P*<0.01.

Table 6 Pearson correlation analysis of the CT with the AL and RNFLT

CT	AL		RNFLT	
	P	*r*	*P*	*r*
CT-N2	<0.0001	-0.414[b]	0.018	-0.141[a]
CT-N1	<0.0001	-0.409[b]	0.009	-0.156[b]
CT-C	<0.0001	-0.386[b]	0.007	-0.161[b]
CT-T2	<0.0001	-0.370[b]	0.008	-0.157[b]
CT-T1	<0.0001	-0.323[b]	0.017	-0.143[a]

CT: Choroidal thickness; AL: Axial length; RNFLT: Retinal nerve fiber layer thickness; T1: Temporal sector 500 μm from the fovea; N1: Nasal sector 500 μm from the fovea; T2: Temporal sector 1000 μm from the fovea; N2: Nasal sector 1000 μm from the fovea; C: Macular fovea. [a]*P*<0.05; [b]*P*<0.01.

aged children remain unclear. Emmetropization is reportedly regulated by visual feedback related to optical defocus and effective refraction. The age of 6y is considered the end of emmetropization, and subsequent eye expansion indicates the beginning of myopia. Later thinning of the CT and extension of the AL set a foundation for myopia, and these factors might establish a foundation for the development of myopia in children[4,30]. Therefore, we designed clinical trials to examine the features of the CT and influencing factors in school-aged children. Our research results show that the average thickness of the choroid in the CT-C region was 264.31±48.93 μm. The CT increased with increasing age from 6 to 10y. The CT at different sites was negatively correlated with age, sex, and RNFLT and positively correlated with the AL, SE, and BMI. Using a Cirrus system, Margolis and Spaide[31] found that the CT in the subfoveal region decreased with increasing age at a rate of 1.56 μm per year. Lau *et al*[7] found that the CT in the subfoveal region was 227.3±42.2 μm using EDI-OCT in the eyes of wearing single-vision spectacles. The differences in the CT among different studies might be attributed to discrepancies in the age, ethnicity, AL and circadian rhythms of the participants. In addition, this study showed that the CT was thicker in the boys compared with the girls, and those with myopia exhibited a thinner choroid than those with emmetropia. These results were consistent with previously reported findings. Clinical studies have indicated that choroidal thinning is closely associated with ever-increasing axial elongation and progressive myopia[32]. We obtained data that firmly support and confirm the assumptions that the axial elongation in myopia is associated with an increased volume of the eyeball, including increases in both the horizontal and vertical diameters. The thinning of the choroid might partially be attributed to morphological changes associated with axial elongation. However, the relationship between the CT and age is ambiguous, and these differences might be due to disparities in the apparatuses and scanning mode of OCT and the refractive error of the volunteers. Fujiwara *et al*[33] and Li *et al*[34] found that the subfoveal CT was closely associated with sex, age and AL in Danish participants. Similar to its relationship to the distance from the macular fovea, the CT might be related to the distance from the optic disc[33-34]. Furthermore, a previous study revealed that the choroid is thickest in those with hyperopia, followed by those with emmetropia, and the choroid is thinnest in the same region in people with myopia[19,35]. Our results are consistent with the CT obtained in a previous study on individuals with low myopia. The accelerated choroidal blood flow produces a high gradient for oxygen diffusion into the outer retina, allows the concentration of metabolic waste products and thereby enhances their removal from the retina[3]. A thicker choroid in the bitemporal area might be closely related to the anatomical structure of the retina. Thinning of the choroid participates in myopic progression, and the CT and AL have been independently associated with myopic shift[13]. Studies have shown that the mRNA levels of the human estrogen receptor, sex and hormone levels might affect choroidal blood flow and thereby affect the CT[36-38]. Animal experiments have demonstrated that the sclera undergoes remodeling during the development of myopia, and scleral choroid ischemia might be one of the targets of myopia. Hyperopic defocus leads to thinning of the choroid, and myopic defocus can give rise to thickening of the choroid[2,39]. Thus, in-depth knowledge of the normal baseline CT is particularly important for the prevention and control of myopia.

Interestingly, the subfoveal CT in amblyopic children is aberrantly high and negatively correlated with the AL. Amblyopia is correlated with a thicker choroid, which might be a potential parameter for future therapeutic directions[40]. Animal models have revealed that the choroid plays a role in emmetropization by secreting multiple growth factors[2]. Some studies have indicated that amblyopia is associated with a thicker subfoveal choroid[41]. Statistical results have shown that in hyperopic anisometropic amblyopia, the CT changes after amblyopia treatment[40]. Similarly, the CT in hyperopic anisometropic amblyopia is clinically thicker than that in control subjects[42]. In summary, the CT in amblyopic eyes is somewhat higher than that in controls. We can assume that the choroid is related to the molecular mechanism of eye growth and the morphological structure of the eye and can thus lead to ametropia. An understanding of the normal baseline CT might provide useful clinical evidence for the diagnosis and treatment of amblyopia.

The current study has several limitations. First, this study was a single-center and cross-sectional investigation. Second, a trend toward a larger bias with thicker CT values was obtained due to the difficulty in assessing the choroid sclera interface in the images. Third, our research indicates that an increasing incidence of myopia is closely associated with the fact that children did not wear glasses after correction of refractive error. Thus, myopic defocus might have induced choroidal thickening. Fourth, we measured only the gross CT and didn't fully consider the various layers of the choroid and the density of the choriocapillaris. Finally, our results might be only applicable to children aged 6-10y. Furthermore, the internal mechanism underlying the relationship between the CT and refractive error is unclear. Further research should focus on the pathogenesis of myopia and the prevention and control of myopia.

The current results have the following clinical significance. First, HD-OCT can be used to measure the retinal thickness

and CT in some eyes of children with a thin choroid, such as those with congenital high myopia. Second, in clinical practice, measurement of the CT in addition to the AL after orthokeratology treatment might provide data support for the prevention and control of myopia. Third, the strengths of our study are expected to encourage follow-up research on the diagnosis and treatment of amblyopia in children. Due to the problems raised in the current study, we should monitor the accuracy and subtle layers of the choroid of the OCT domain.

Our cross-sectional study provides demographic data and an understanding of the normal baseline features of ocular parameters. The results showed that the CT is mildly inversely correlated with age, sex and AL and positively correlated with the SE and BMI. We will follow the cohort of participants uninterruptedly, which might help us provide an in-depth explanation of the role of the choroid. To verify this speculation and make certain changes in the CT with time elapse, larger sample sizes, longer linear scan lengths, wide-field CT maps of the posterior pole and the precision of instrument measurement will be considered. The myopic eye itself presents challenges due to its irregular shape and anatomical distortion of the posterior segment layers, which can affect evaluation of the images produced. Thus, further studies are needed to improve the techniques used for ocular imaging and prove whether thickening of the choroid plays an indispensable role in the pathogenesis of myopia and the prevention and control of myopia.

In conclusion, we established demographic information for the choroid and RNFLT, and these findings provide information that should be considered in future analyses of the CT and RNFLT in OCT studies in school-aged children.

ACKNOWLEDGEMENTS

Authors' contributions: Wang CX participated in the conception and design of the research study. All the authors contributed to the collection of the data and the statistical analyses of the data. Liu WQ and Wang CX wrote and revised the manuscript.

Foundations: Supported by Zhejiang Province University Student Planted Talent Plan (No.2015R413023); Public Welfare Social Development Science and Technology Project of Wenzhou Science and Technologies Bureau (No. Y20160443).

Conflicts of Interest: Liu WQ, None; **Wang DD,** None; **Yang XX,** None; **Pan YY,** None; **Song X,** None; **Hou YS,** None; **Wang CX,** None.

REFERENCES

1 Tan CS, Ngo W, Cheong KX. Comparison of choroidal thicknesses using swept source and spectral domain optical coherence tomography in diseased and normal eyes. *Br J Ophthalmol* 2014; 99(3):354-358.

2 Wu H, Chen W, Zhao F, *et al*. Scleral hypoxia is a target for myopia control. *Proc Natl Acad Sci U S A* 2018;115(30):E7091-E7100.

3 Nickla DL, Wallman J. The multifunctional choroid. *Prog Retin Eye Res* 2010;29:144-168.

4 Ang M, Wong CW, Hoang QV, Cheung GCM, Lee SY, Chia A, Saw SM, Ohno-Matsui K, Schmetterer L. Imaging in myopia: potential biomarkers, current challenges and future developments. *Br J Ophthalmol* 2019;103(6):855-862.

5 Rudnicka AR, Kapetanakis VV, Wathern AK, *et al*. Global variations and time trends in the prevalence of childhood myopia, a systematic review and quantitative meta-analysis: implications for aetiology and early prevention. *Br J Ophthalmol* 2016;100:882-890.

6 Holden BA, Fricke TR, Wilson DA, Jong M, Naidoo KS, Sankaridurg P, Wong TY, Naduvilath TJ, Resnikoff S. Global prevalence of myopia and high myopia and temporal trends from 2000 through 2050. *Ophthalmology* 2016;123(5):1036-1042.

7 Lau JK, Cheung SW, Collins MJ, Cho P. Repeatability of choroidal thickness measurements with Spectralis OCT images. *BMJ Open Ophthalmol* 2019;4(1):e000237.

8 Branchini L, Regatieri CV, Flores-Moreno I, Baumann B, Fujimoto JG, Duker JS. Reproducibility of choroidal thickness measurements across three spectral domain optical coherence tomography systems. *Ophthalmology* 2012;119(1):119-123.

9 Chhablani J, Barteselli G, Wang HY, El-Emam S, Kozak I, Doede AL, Bartsch DU, Cheng LY, Freeman WR. Repeatability and reproducibility of manual choroidal volume measurements using enhanced depth imaging optical coherence tomography. *Invest Ophthalmol Vis Sci* 2012;53(4):2274-2280.

10 Nagasawa T, Mitamura Y, Katome T, Shinomiya K, Naito T, Nagasato D, Shimizu Y, Tabuchi H, Kiuchi Y. Macular choroidal thickness and volume in healthy pediatric individuals measured by swept-source optical coherence tomography. *Invest Ophthalmol Vis Sci* 2013;54(10):7068-7074.

11 Gaier ED, Gise R, Heidary G. Imaging amblyopia: insights from optical coherence tomography (OCT). *Semin Ophthalmol* 2019;34(4):303-311.

12 Araki S, Miki A, Goto K, Yamashita T, Takizawa G, Haruishi K, Ieki Y, Kiryu J, Yaoeda K. Macular retinal and choroidal thickness in unilateral amblyopia using swept-source optical coherence tomography. *BMC Ophthalmol* 2017;17(1):167.

13 Jin PY, Zou HD, Xu X, Chang TC, Zhu JF, Deng JJ, Lv M, Jin JL, Sun SF, Wang L, He XG. Longitudinal changes in choroidal and retinal thicknesses in children with myopic shift. *Retina* 2019;39(6):1091-1099.

14 Kong MG, Choi DY, Han G, Song YM, Park SY, Sung J, Hwang S, Ham DI. Measurable range of subfoveal choroidal thickness with conventional spectral domain optical coherence tomography. *Transl Vis Sci Technol* 2018;7(5):16.

15 Brautaset R, Birkeldh U, Rosén R, Ramsay MW, Nilsson M. Reproducibility of disc and macula optical coherence tomography

using the Canon OCT-HS100 as compared with the Zeiss Cirrus HD-OCT. *Eur J Ophthalmol* 2014;24(5):722-727.

16 Brennen PM, Kagemann L, Friberg TR. Comparison of StratusOCT and cirrus HD-OCT imaging in macular diseases. *Ophthalmic Surg Lasers Imaging* 2009;40(1):25-31.

17 Ostrin LA, Jnawali A, Carkeet A, Patel NB. Twenty-four hour ocular and systemic diurnal rhythms in children. *Ophthalmic Physiol Opt* 2019;39(5):358-369.

18 Moderiano D, Do M, Hobbs S, Lam V, Sarin S, Alonso-Caneiro D, Chakraborty R. Influence of the time of day on axial length and choroidal thickness changes to hyperopic and myopic defocus in human eyes. *Exp Eye Res* 2019;182:125-136.

19 He XG, Jin PY, Zou HD, Li QQ, Jin JL, Lu LN, Zhao HJ, He JN, Xu X, Wang MJ, Zhu JF. Choroidal thickness in healthy chinese children aged 6 to 12: the Shanghai children eye study. *Retina* 2017;37(2):368-375.

20 Jin PY, Zou HD, Zhu JF, Xu X, Jin JL, Chang TC, Lu LN, Yuan H, Sun SF, Yan B, He JN, Wang MJ, He XG. Choroidal and retinal thickness in children with different refractive status measured by swept-source optical coherence tomography. *Am J Ophthalmol* 2016;168:164-176.

21 Park KA, Oh SY. Choroidal thickness in healthy children. *Retina* 2013;33(9):1971-1976.

22 Ruiz-Moreno JM, Flores-Moreno I, Lugo F, Ruiz-Medrano J, Montero JA, Akiba M. Macular choroidal thickness in normal pediatric population measured by swept-source optical coherence tomography. *Invest Ophthalmol Vis Sci* 2013;54(1):353-359.

23 Zhang JM, Wu JF, Chen JH, Wang L, Lu TL, Sun W, Hu YY, Jiang WJ, Guo DD, Wang XR, Bi HS, Jonas JB. Macular choroidal thickness in children: the Shandong children eye study. *Invest Ophthalmol Vis Sci* 2015;56(13):7646-7652.

24 Kase S, Endo H, Takahashi M, Saito M, Yokoi M, Ito Y, Katsuta S, Sonoda S, Sakamoto T, Ishida S, Kase M. Alteration of choroidal vascular structure in diabetic retinopathy. *Br J Ophthalmol* 2019.

25 Pongsachareonnont P, Somkijrungroj T, Assavapongpaiboon B, Chitamara T, Chuntarapas M, Suwajanakorn D. Foveal and parafoveal choroidal thickness pattern measuring by swept source optical coherence tomography. *Eye (Lond)* 2019;33(9):1443-1451.

26 Ho M, Liu DT, Chan VC, Lam DS. Choroidal thickness measurement in myopic eyes by enhanced depth optical coherence tomography. *Ophthalmology* 2013;120(9):1909-1914.

27 Chhablani JK, Deshpande R, Sachdeva V, Vidya S, Rao PS, Panigati A, Mahat B, Pappuru RR, Pehere N, Pathengay A. Choroidal thickness profile in healthy Indian children. *Indian J Ophthalmol* 2015;63(6):474-477.

28 Wei WB, Xu L, Jonas JB, *et al*. Subfoveal choroidal thickness: the Beijing Eye Study. *Ophthalmology* 2013;120:175-180.

29 Deng JJ, Jin JL, Lv M, Jiang WH, Sun SF, Yao CX, Zhu JF, Zou HD, Wang L, He XG, Xu X. Distribution of scleral thickness and associated factors in 810 Chinese children and adolescents: a swept-source optical coherence tomography study. *Acta Ophthalmol* 2019;97(3):e410-e418.

30 Hoseini-Yazdi H, Vincent SJ, Collins MJ, Read SA, Alonso-Caneiro D. Wide-field choroidal thickness in myopes and emmetropes. *Sci Rep* 2019;9(1):3474.

31 Margolis R, Spaide RF. A pilot study of enhanced depth imaging optical coherence tomography of the choroid in normal eyes. *Am J Ophthalmol* 2009;147(5):811-815.

32 Fang YX, Du R, Nagaoka N, Yokoi T, Shinohara K, Xu X, Takahashi H, Onishi Y, Yoshida T, Ohno-Matsui K. OCT-based diagnostic criteria for different stages of myopic maculopathy. *Ophthalmology* 2019;126(7):1018-1032.

33 Fujiwara A, Shiragami C, Shirakata Y, Manabe S, Izumibata S, Shiraga F. Enhanced depth imaging spectral-domain optical coherence tomography of subfoveal choroidal thickness in normal Japanese eyes. *Jpn J Ophthalmol* 2012;56(3):230-235.

34 Li XQ, Larsen M, Munch IC. Subfoveal choroidal thickness in relation to sex and axial length in 93 Danish university students. *Invest Ophthalmol Vis Sci* 2011;52(11):8438-8441.

35 Deng JJ, Li XL, Jin JL, *et al*. Distribution pattern of choroidal thickness at the posterior pole in Chinese children with myopia. *Invest Ophthalmol Vis Sci* 2018;59:1577-1586.

36 Centofanti M, Bonini S, Manni G, Guinetti-Neuschüler C, Bucci MG, Harris A. Do sex and hormonal status influence choroidal circulation? *Br J Ophthalmol* 2000;84(7):786-787.

37 Munaut C, Lambert V, Noël A, Frankenne F, Deprez M, Foidart JM, Rakic JM. Presence of oestrogen receptor type beta in human retina. *Br J Ophthalmol* 2001;85(7):877-882.

38 Kavroulaki D, Gugleta K, Kochkorov A, Katamay R, Flammer J, Orgul S. Influence of gender and menopausal status on peripheral and choroidal circulation. *Acta Ophthalmol* 2010;88(8):850-853.

39 Hoseini-Yazdi H, Vincent SJ, Collins MJ, Read SA. Regional alterations in human choroidal thickness in response to short-term monocular hemifield myopic defocus. *Ophthalmic Physiol Opt* 2019;39(3):172-182.

40 Aslan Bayhan S, Bayhan HA. Effect of amblyopia treatment on choroidal thickness in children with hyperopic anisometropic amblyopia. *Curr Eye Res* 2017;42(9):1254-1259.

41 Hansen MH, Munch IC, Li XQ, Skovgaard AM, Olsen EM, Larsen M, Kessel L. Visual acuity and amblyopia prevalence in 11- to 12-year-old Danish children from the Copenhagen Child Cohort 2000. *Acta Ophthalmol* 2019;97(1):29-35.

42 Öner V, Bulut A, Büyüktarakçı Ş, Kaim M. Influence of hyperopia and amblyopia on choroidal thickness in children. *Eur J Ophthalmol* 2016;26(6):623-626.